Flow field in the compressor blade cascade NACA 65-100

Tomáš Turek

Thesis Supervisor: Ing. Tomáš Hyhlík, Ph.D.

Abstract

An investigation is made into the effects of a flow field in the compressor blade cascade NACA 65-100. This task has two main sections to explore, the transonic flow and the transition model. These sections are solving via the CFD software ANSYS Fluent. The transonic flow with compressible fluid and with steady flow is solving by the RNG k-ε model with non-equilibrium wall functions. Shock waves for the transonic flow are found by choosing the supersonic Mach number and adapted. The transition model is without an effect of compressibility and is consists of the laminar flow and the turbulent flow. Shock waves are eliminated for the transition model by choosing the subsonic Mach number. The laminar flow with incompressible fluid and with unsteady flow is solving by the laminar model. The turbulent flow with incompressible fluid and with steady flow is solving by the standard model and after by the advance model. The standard model is the RNG k-ε model with non-equilibrium wall functions and the advance model is the SST transition model.

Keywords

Flow field, NACA 65-100, transonic flow, transition model, laminar flow, turbulent flow, ANSYS Fluent, laminar model, RNG k-ε model, SST transition model, boundary layer, Mach number, shock wave, adaptation, separation, transition, bypass transition.

1. Introduction

The National Advisory Committee for Aeronautics (*NACA*) [5] was a U.S. federal agency founded in 1915 with the intent to support and perform an aeronautical research. The *NACA* was dissolved in 1958 and passed the torch to newly created National Aeronautics and Space Administration (*NASA*). Parts of the *NACA* are still being used in new designs, e.g., *NACA airfoils* which are airfoils shapes for aircraft wings, *NACA cowling* which is a type of aerodynamics fairing use to streamline of radial engines for airplanes or the *NACA duct* which is a type of the low-drag intake design mostly used for the automotive industry.

Motion of process in devices which are using blades for their function to deliver fluids, air, etc., such as turbines and blade devices depends on a proper shape of blades. On a shape of blades depends a flow field and consequently on it a final efficiency of the whole process. To find if the given shape of a blade is used the most effectively we need take out the characteristic section of a blade, so called the blade cascade section *Fig. 1* which will be computed and consequently reviewed.

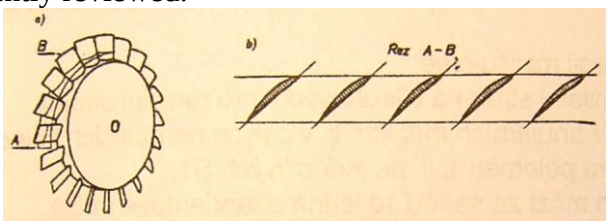

Fig. 1. *The blade cascade section [3].*

An investigation of blade cascades can be performed experimentally, e.g., by measuring in aerodynamic tunnels and also by *PIV* or computationally by *CFD*. Measurement of blade cascades in aerodynamic tunnels is the oldest method and is used to gain lots of information, e.g., characteristics of blade cascades and prototypes, losses, output angles, 3D flow field or the verification of *CFD* methods. The particle image velocimetry method (*PIV*) is the newest method of measuring a field of instantaneous velocities but to determine a track of particles is a very difficult problem dealing with a structure of turbulence and also with a hardware and with a software. The computational fluid dynamics (*CFD*) uses computers to perform calculations of numerical methods and algorithms to describe flowing.
Two of basic problems [3] *AP* and *DP* have been described to create a blade cascade. The analysis problem (*AP)* can be solving by experimental methods, e.g., in an aerodynamic tunnel or by *PIV* method or by a computation method with *CFD*. The design problem (*DP*) is solving by *CFD* and is the inverted method of *AP*, i.e., an optimal shape of a blade cascade with required aerodynamics properties is searching for the given speed triangle and the arrangement of velocity in the profile.

2. Formulation

2.1 Conditions

The profile of a compressor blade cascade is the NACA 65-100 with a strengthened trailing edge [1] obtained from the Academy of Science of the Czech Republic. Basic geometric quantities of the profile *Fig. 2* are included in the documentation [1], e.g., an angle of the profile setting $\gamma = 17$ [°], an angle of incoming flow $\alpha_{1,ref} = 45.8$ [°], a profile chord c = 80 [mm] and spacing s = 40 [mm].

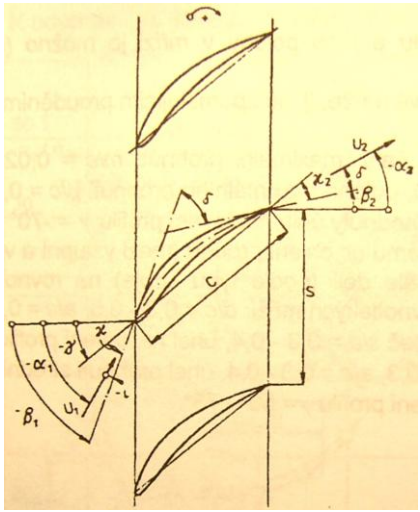

Fig. 2. *Basic angles of the profile [3].*

The flowing medium in a blade cascade is air. Flow is steady and two dimensional. Viscid and a compressible liquid are expected.
It was used the *AP* and the *CFD* method. Creating of geometry and a mesh were implemented by *Gambit* followed by adjusting a mesh by *TGrid*. A computation was accomplished by *ANSYS Fluent*.

2.2 Basic solving methods

Numerical solving of a flow field with *CFD* by *ANSYS Fluent* for compressible flows is used the *implicit* and the *explicit method* [1]:

a) *Implicit method:* For a given variable, the unknown value in each cell is computed by using a relation that includes both existing and unknown values from neighboring cells. Therefore each unknown will appear in more than one equation in the system, and these equations must be solved simultaneously to give the unknown.
b) *Explicit method:* For a given variable, the unknown value in each cell is computed by using a relation that includes only the existing values. Therefore each unknown will appear in only one equation in the system and the equations for the unknown value in each cell can be solved one at a time to give the unknown quantities.

To solve the hyperbolic partial differential equations in *ANSYS Fluent* are used the *Upwind* schemes which denote a class of numerical discretization methods:

i) *First order upwind:* is using when previous results are unknown.
ii) *Second order upwind:* is replacing the first derivation in second class of accuracy and faces to a greater result. Not only the value of zero in a cell against to direction of velocity is using, also its own derivation which is determine from a flow through walls.

3. Procedure

3.1 Creating a mesh

The basis to creation of the geometry [1] was obtained from the Institute of Thermomechanics of the ASCR, v. v. i., in a form of the documentation for a future experiment.
In the graphics pre-processor *Gambit v6.3* was created the given profile of a blade cascade. Points of the geometry were transferred from a text editor and consequently sketched in of the leading and the trailing edge of the flowed profile. The profile had been divided on the upper and the lower part.

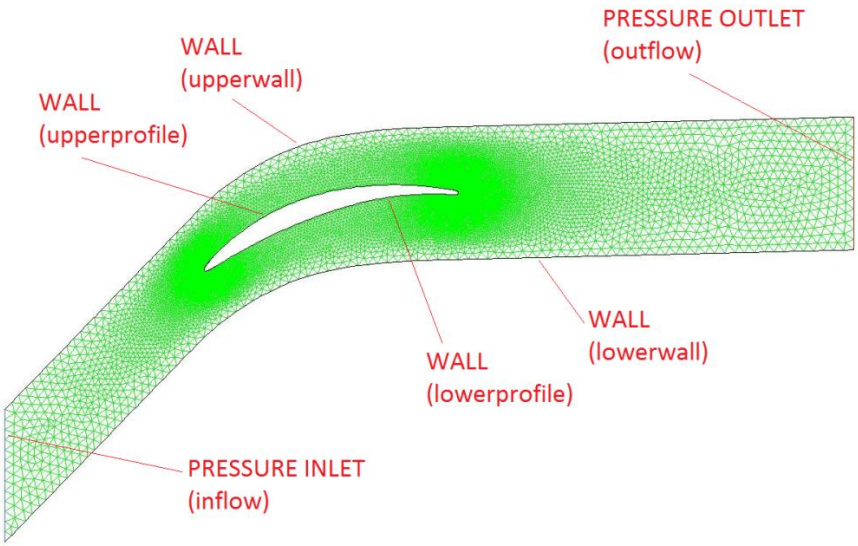

Fig. 3. *Boundary conditions for the created geometry with the modified mesh (in brackets are noted names for individual parts which were used in the program).*

The geometry was made and boundary conditions *Fig. 3* were associated on it. On the flowed profile was made a boundary layer.
The mesh was suitable applied to the created geometry with regard to the blade cascade profile. The mesh was examined by evaluative factors: *aspect ratio* (values to 0.5), *size change* (to 1.5), and *equisize skew* (to 0.5). Consequently the mesh was modified to pass these

factors, whereas the best values of factors must be reached at the leading and the trailing edge of the flowed profile.
The generator *TGrid v4.0* had been used in order to improve *skewnees*, which wasn't met by *equisize skew* in the pre-processor *Gambit*. Skewness was calculated on the mesh imported from *Gambit*. The demanded value was reached.
The modified mesh *Figs. 3, 5* passed all evaluative factors and was prepared for a computation.

3.2 Setting of a computational model

The setting and the computation of a blade cascade were accomplished in the program *ANSYS Fluent v12*, which using the general conservation equations [2] to solve *CFD* – the mass conservation equation (1. 1), the momentum conservation equation (1. 2) and the energy conservation equation (1. 3).

$$\frac{\partial \rho}{\partial t} + \nabla . \left(\rho . \vec{v} \right) = S_m \tag{1. 1}$$

$$\frac{\partial}{\partial t} . \left(\rho . \vec{v} \right) + \nabla . \left(\rho . \vec{v} . \vec{v} \right) = -\nabla p + \nabla . \overline{\overline{(\tau)}} + \rho . \vec{g} + \vec{F} \tag{1. 2}$$

$$\frac{\partial}{\partial t} . \left(\rho . E \right) + \nabla . \left(\vec{v} . \left(\rho . E + p \right) \right) = \nabla . \left(k_{eff} . \nabla T - \sum_j h_j . \overrightarrow{J_j} + \left(\overline{\overline{\tau_{eff}}} . \vec{v} \right) \right) + S_h \tag{1. 3}$$

Equations are solved as a system of partial equations using the finite volume method. *ANSYS Fluent* solves compressible flows in the form of equations which are listed above. For various types of flows these equations are converting to the specific forms.
The mesh is imported from *TGrid* to *ANSYS Fluent*, where are set up boundary conditions for a computation, e.g., a direction vector of an entry angle of a flow, pressure on the input and the output or temperature.
Periodic conditions are assigned for the upper and the lower wall by printing in a text menu whereby the one wall is eliminated.
The computation of the pressure on the output (2. 2) by the Mach number [4] for the transition model:

$$M = \frac{c}{a} = \frac{\sqrt{\frac{2 . \kappa . r}{\kappa - 1} . \left(T_0 - T \right)}}{\sqrt{\kappa . r . T}} = \sqrt{\frac{2}{\kappa - 1} . \left(\frac{T_0}{T} - 1 \right)} = \sqrt{\frac{2}{\kappa - 1} . \left[\left(\frac{p}{p_0} \right)^{\frac{1-\kappa}{\kappa}} - 1 \right]} \tag{2. 1}$$

$$M = \sqrt{\frac{2}{\kappa - 1} . \left[\left(\frac{p}{p_0} \right)^{\frac{1-\kappa}{\kappa}} - 1 \right]} \quad \Rightarrow \quad p = p_0 . \left(M^2 . \frac{\kappa - 1}{2} + 1 \right)^{\frac{\kappa}{1-\kappa}} \tag{2. 2}$$

$$p = 100000 . \left(0{,}2^2 . \frac{1{,}4 - 1}{2} + 1 \right)^{\frac{1{,}4}{1-1{,}4}} = \underline{\underline{97250 \left[Pa \right]}}$$

I. <u>*The transonic flow:*</u> Since the liquid is compressible the *density based* method is used. The ideal gas is associated for the behavior of air. The energy model and the robust model *RNG k-ε* with non-equilibrium wall functions were chosen. The pressure mode

is 0.8. The pressure on the input p_0 = 100000 [Pa], the pressure on the output p = 80000 [Pa] and the temperature T_0 = 300 [K] are set up.

II. *The transition model:* Since the liquid is incompressible the *pressure based* method is used. The constant is associated for the behavior of air. The Mach number is chosen M = 0.2 [-] and for it is computed the pressure on the output (2. 2), so that the mode without shock waves can be expected. The pressure mode is 0.97. The pressure on the input p_0 = 100000 [Pa] and the computed pressure on the output p = 97000 [Pa] are set up.

3.3 Computation

Firstly is computed with the first order upwind and after with the second order upwind when a computation is performed by schemes. Confirmation that all of conditions are correct and can be used for next computations is the fact that residues become steady after each of scheme. The double precision option in a start of *ANSYS Fluent* was chose in purpose to decline residues so that to gain better results.

I. *The transonic flow:* The implicit method and the scheme of first order upwind were chosen. The computation was initialized by set up of parameters and the model was computed just in order to know if the residues don't start diverge. If the residues after a computation had tendency be steady, converge, the explicit method and the second order upwind scheme is chosen. From graphics outputs is found an area where is occur a shock wave. This area is important for a computation because there is a change of velocity. So we endeavor to refine the mesh in the area of the shock wave in order to get better results. We obtain that by adaptations with a proper selection of a threshold in order to select not so many cells abreast. Cells can't lie next to each other, it must be at the most just a one row of cells variously oriented by vertically, horizontally or another directions. Only cells in a specific area are adapted so that a computation isn't burdened. Adaptations over density, pressure, velocity and boundary were performed till was worth it to adapt given cells.

II. *The transition model:* For the laminar flow the fractional step scheme and standard method for pressure were chosen. The time step size was computed from a dimension of cells divided by velocity. For the standard method and the advance method of the turbulent flow the simple scheme and the standard method for pressure were chosen.

4. Comparison

Graphics outputs were made after the computation and they represent reached results on the computational model. These graphics outputs are used for comparison of an effect of individual changes with supposed results or values reached by the computation.

4.1 The transonic flow

The computation of the Mach number [4] on the output (3):

$$M = \sqrt{\frac{2}{\kappa - 1} \cdot \left[\left(\frac{p}{p_0} \right)^{\frac{1-\kappa}{\kappa}} - 1 \right]} = \sqrt{\frac{2}{1.4 - 1} \cdot \left[\left(\frac{80000}{100000} \right)^{\frac{1-1.4}{1.4}} - 1 \right]} = \underline{\underline{0{,}574\,[-]}} \qquad (3)$$

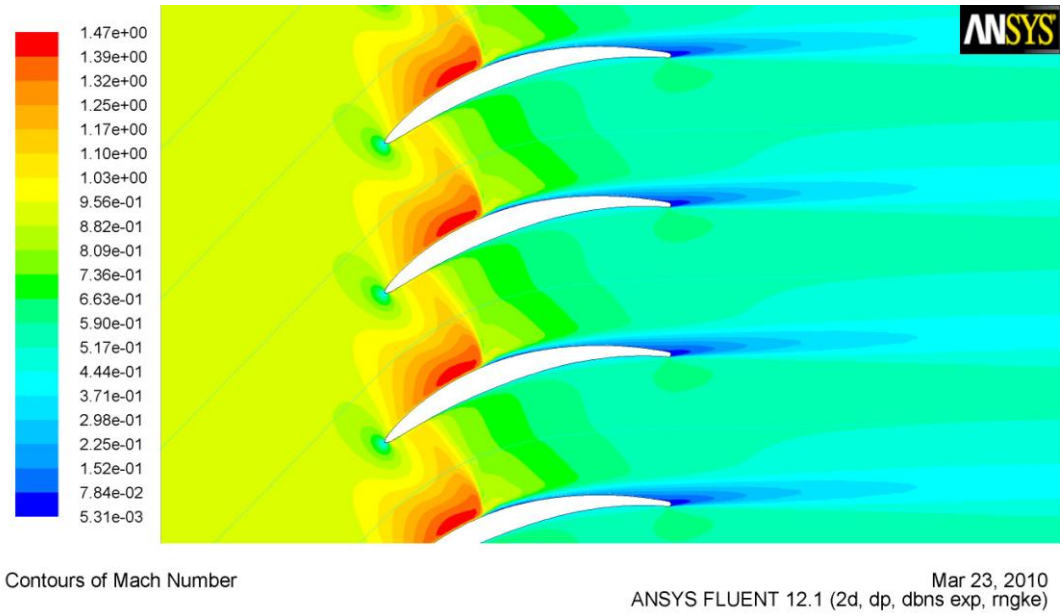

Fig. 4. *Contours of the Mach number in the compressor blade cascade NACA 65-100.*

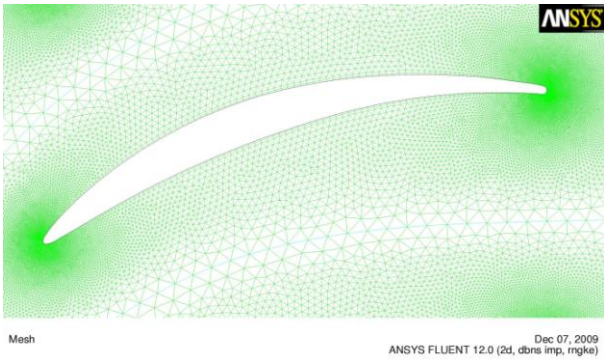

Fig. 5. *The computational mesh before applying adaptations.*

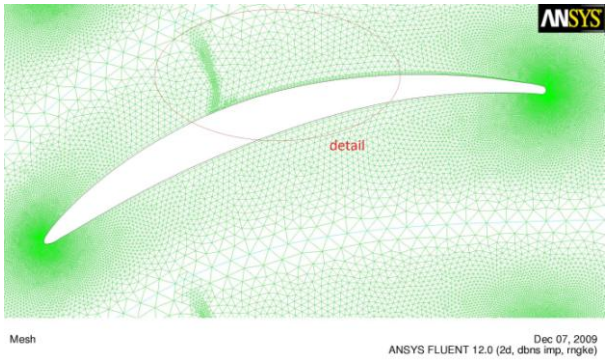

Fig. 6. *The computational mesh after adaptations.*

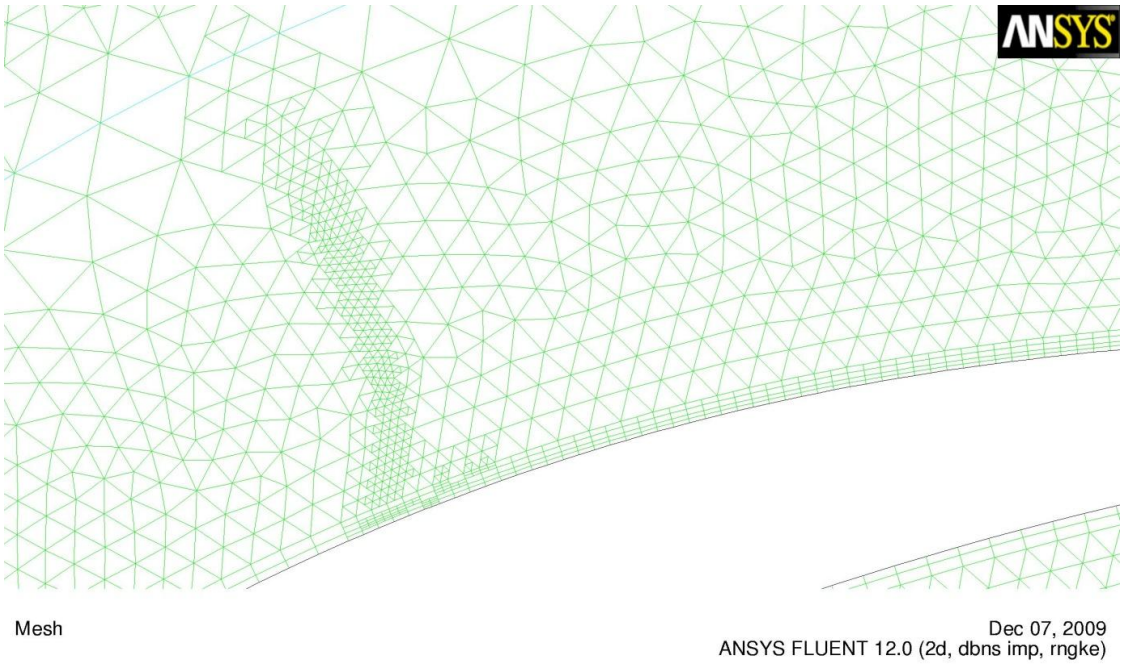

Fig. 7. *The detail of the computational mesh after adaptations.*

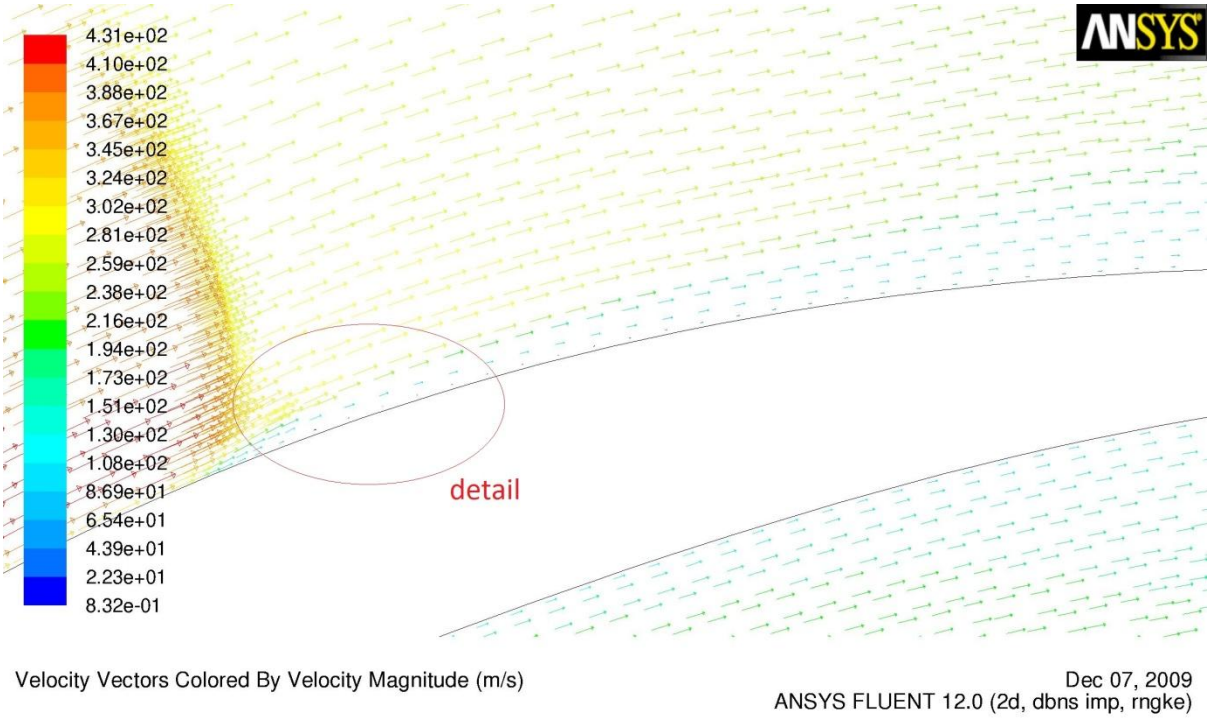

Fig. 8. *The behavior of velocity represented by vectors after adaptations around the shock wave.*

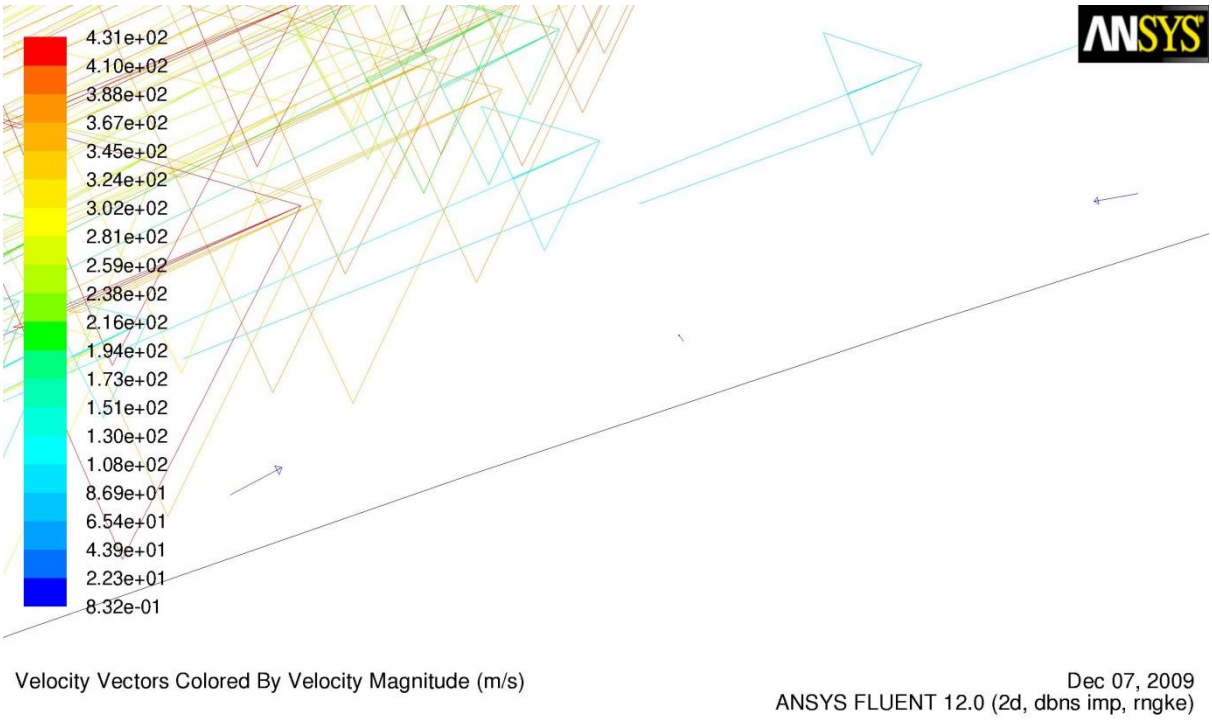

Fig. 9. *The detail of the behavior of velocity represented by vectors after adaptations around the shock wave.*

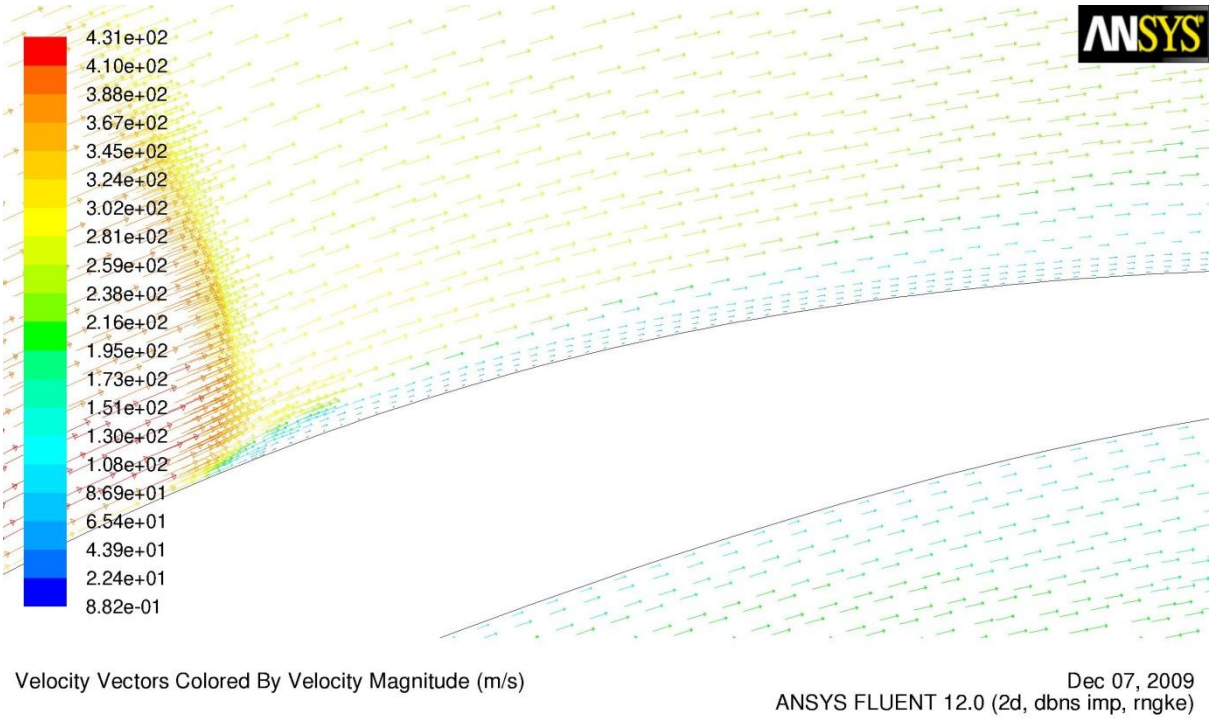

Fig. 10. *The behavior of velocity represented by vectors after the adaptation over boundary in the boundary layer.*

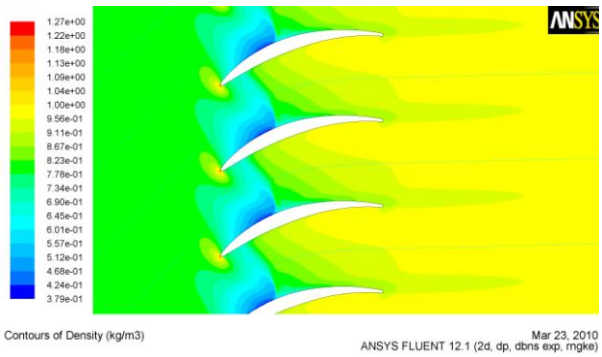

Fig. 11. *Contours of density in the compressor blade cascade.*

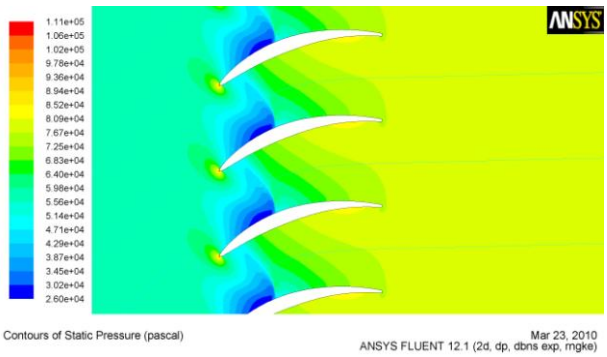

Fig. 12. *Contours of statistic pressure in the compressor blade cascade.*

4.2 The transition model

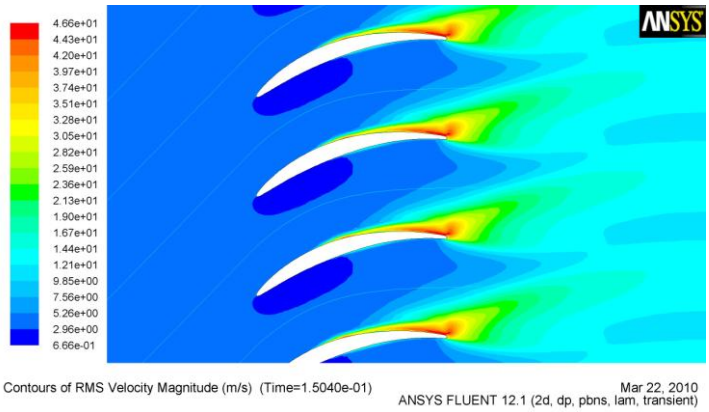

Fig. 13. *The laminar flow – contours of RMS velocity magnitude in the compressor blade cascade.*

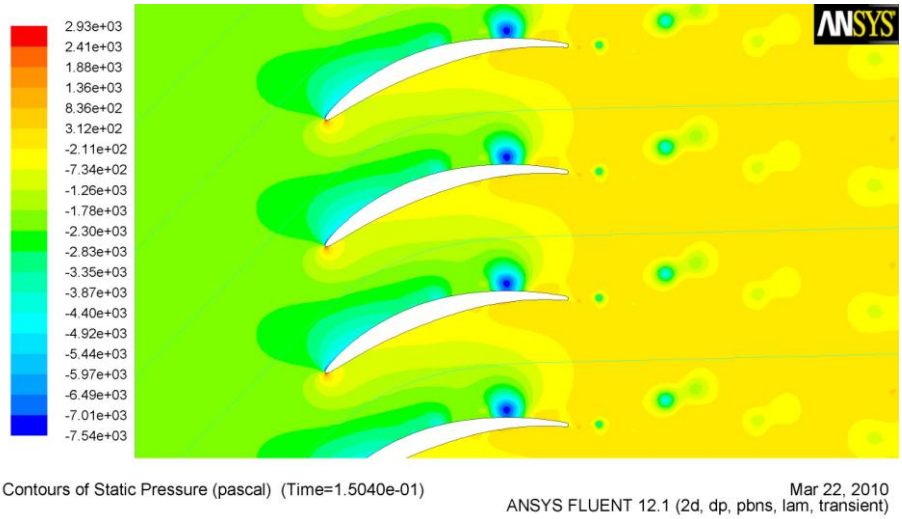

Fig. 14. *The laminar flow – contours of static pressure in the compressor blade cascade.*

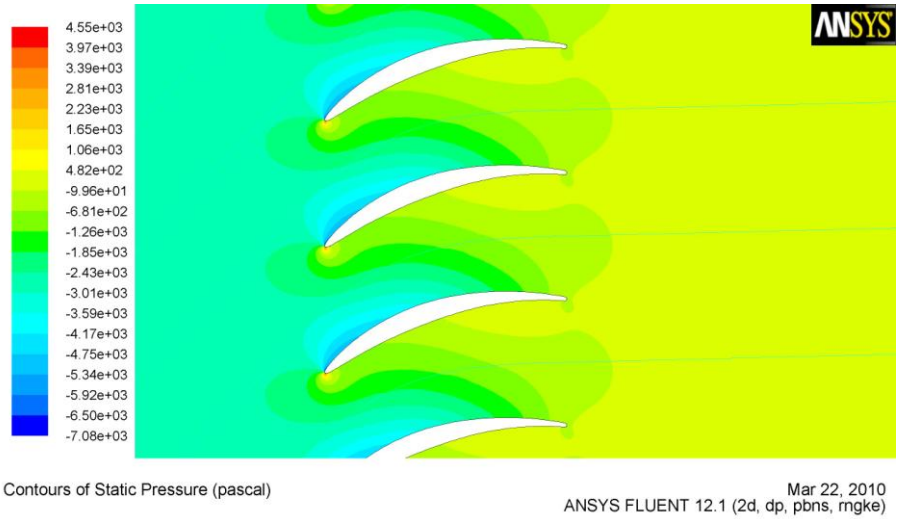

Fig. 15. *The turbulent flow of the standard model – contours of static pressure in the compressor blade cascade.*

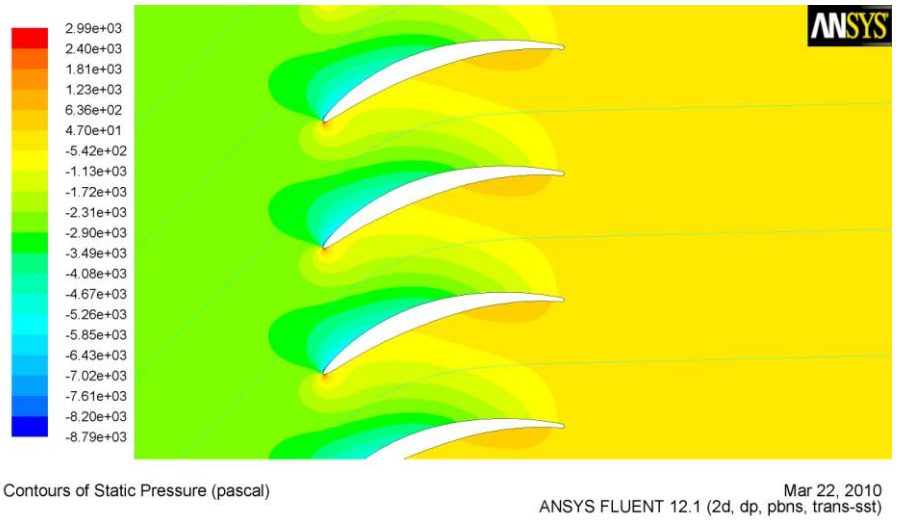

Fig. 16. *The turbulent flow of the advanced model – contours of static pressure in the compressor blade cascade.*

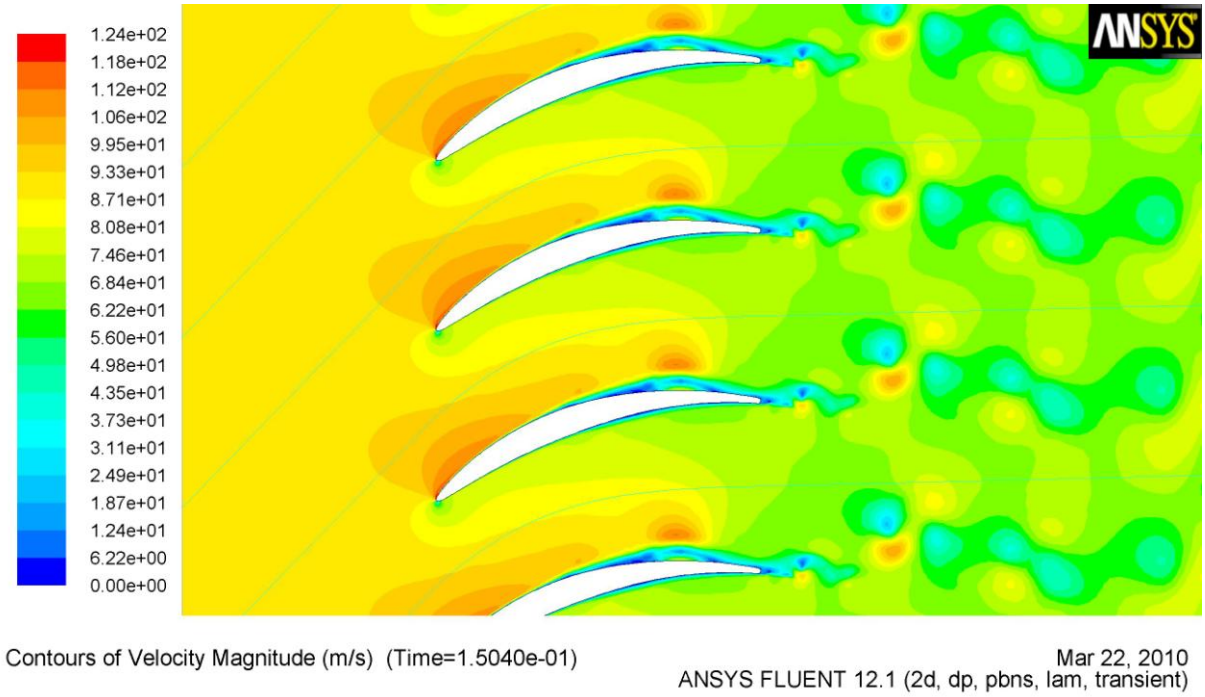

Fig. 17. *The laminar flow – contours of velocity magnitude in the compressor blade cascade.*

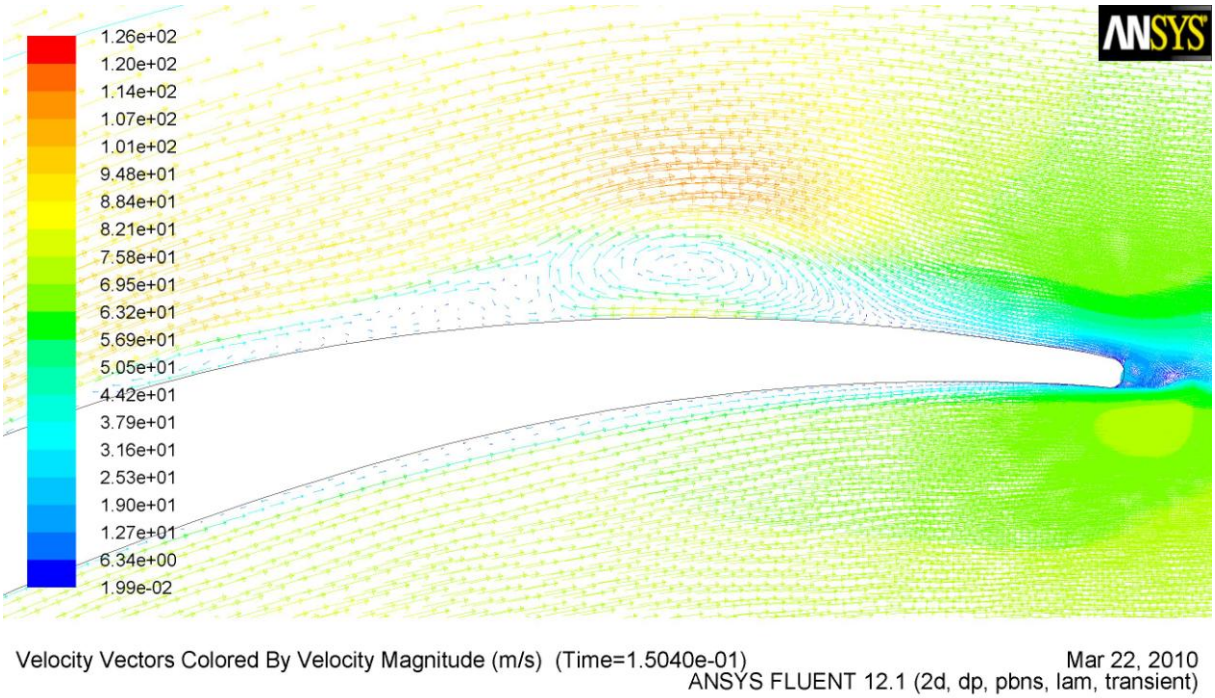

Fig. 18. *The laminar flow – the behavior of velocity represented by vectors nearby trailing edge in the compressor blade cascade.*

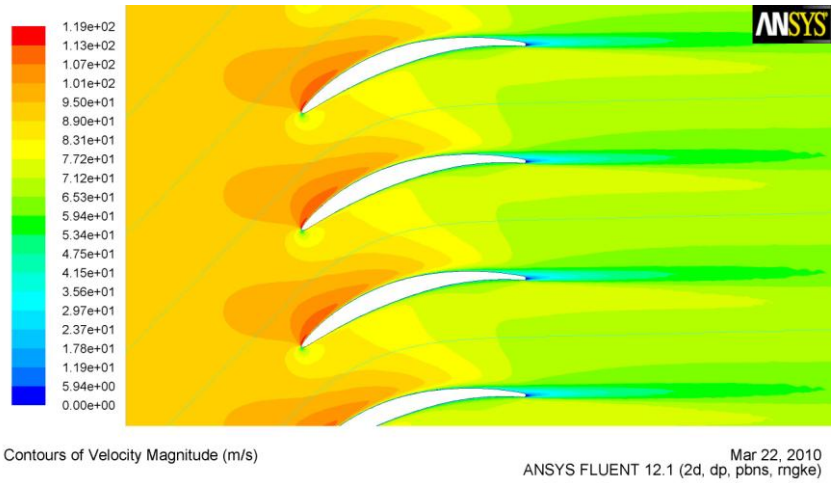

Fig. 19. *The turbulent flow of the standard model – contours of velocity magnitude in the compressor blade cascade.*

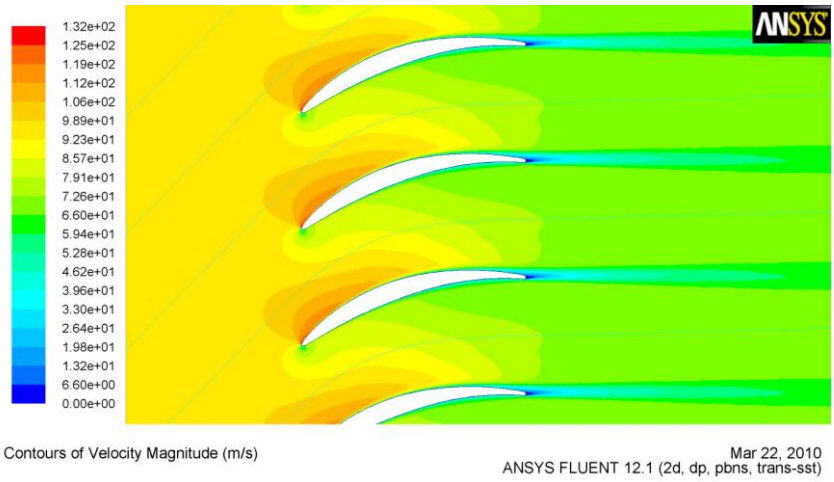

Fig. 20. *The turbulent flow of the advance model – contours of velocity magnitude in the compressor blade cascade.*

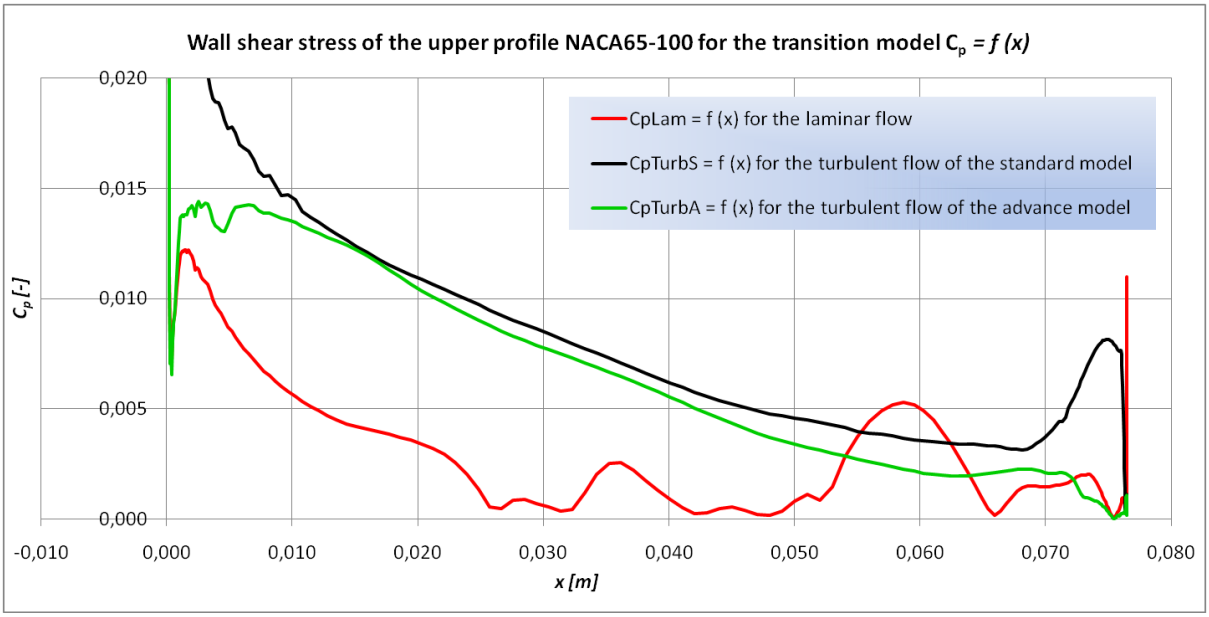

Fig. 21. *The transition model - wall shear stress of the upper profile NACA 65-100.*

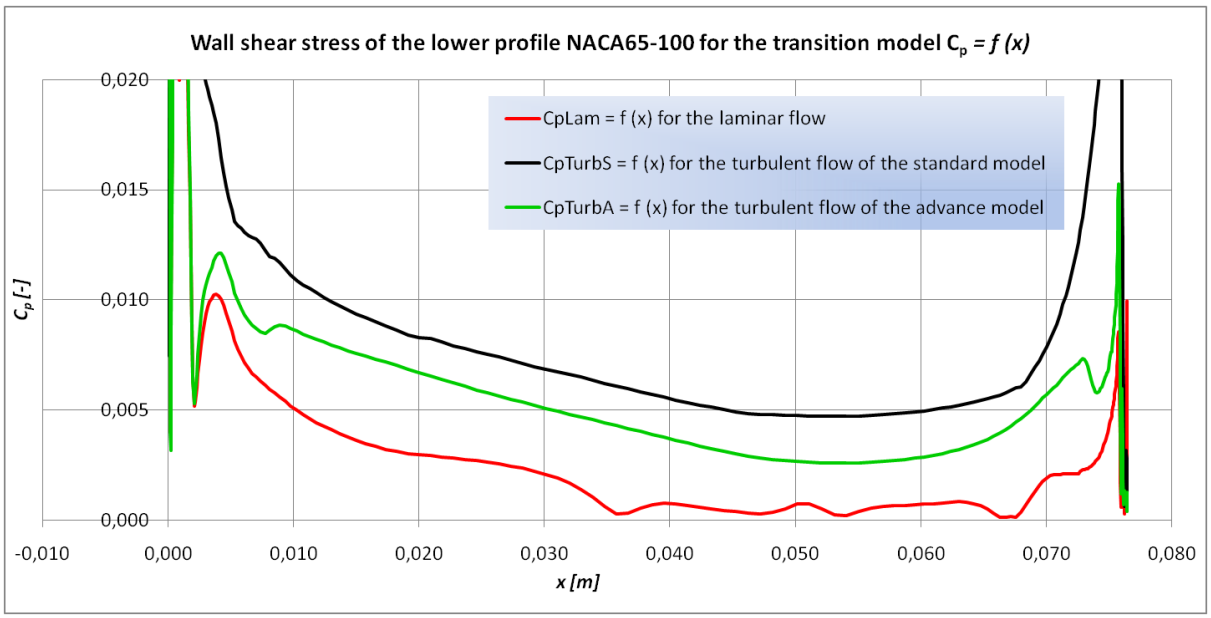

Fig. 22. *The transition model - wall shear stress of the lower profile NACA 65-100.*

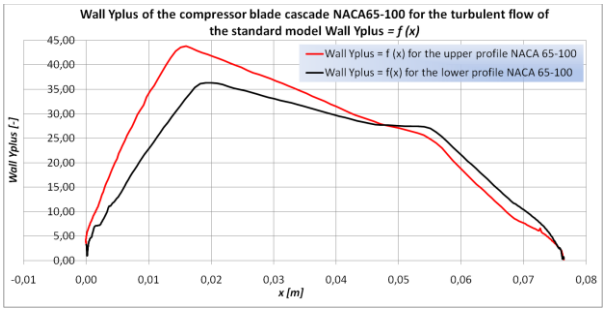

Fig. 23. *The turbulent flow of the standard model – Wall Yplus of the NACA 65-100.*

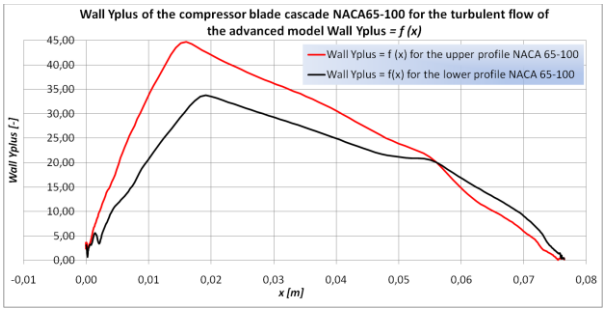

Fig. 24. *The turbulent flow of the advance model – Wall Yplus of the NACA 65-100.*

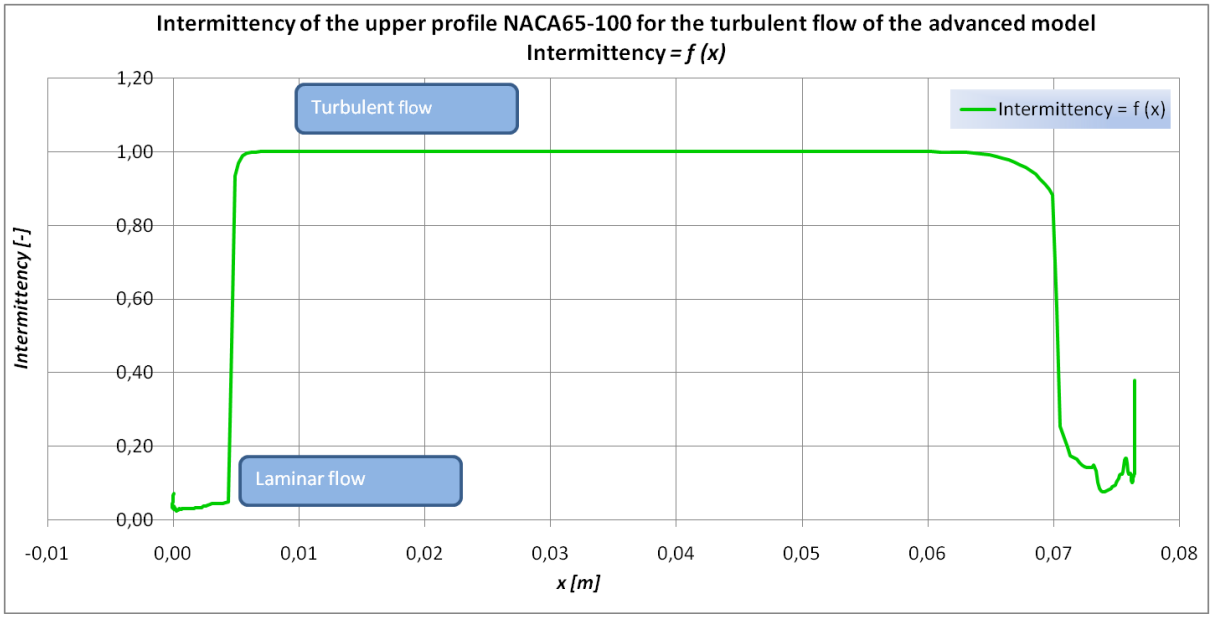

Fig. 25. *The turbulent flow with the advance model – intermittency of the upper profile NACA 65-100.*

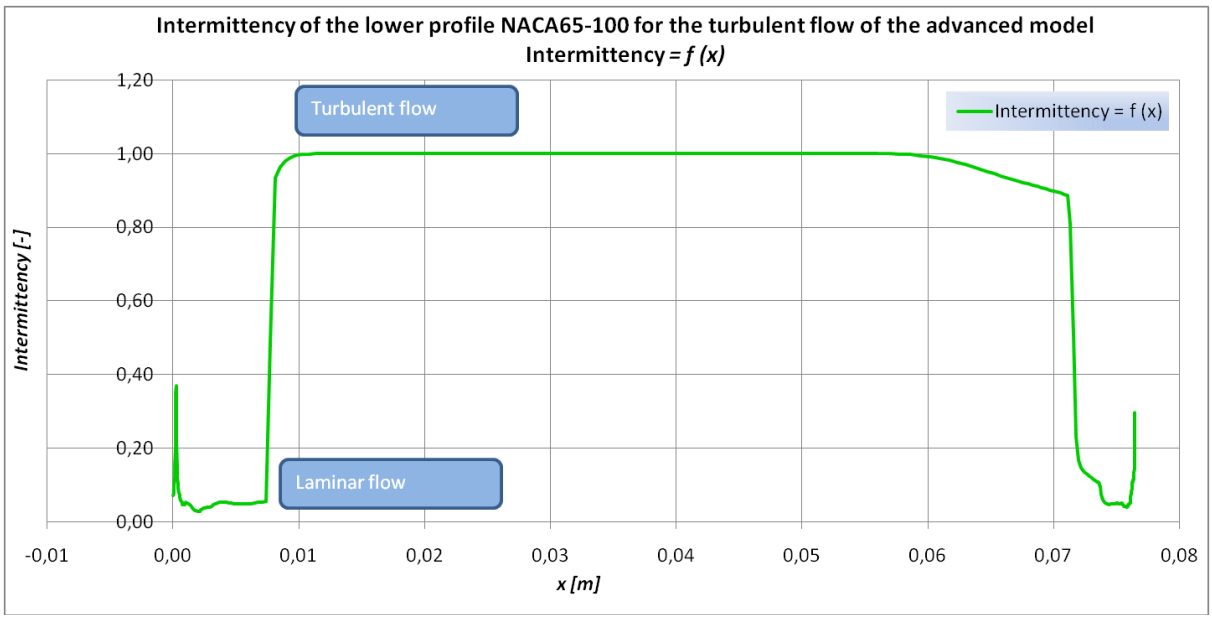

Fig. 26. *The turbulent flow with the advance model – intermittency of the lower profile NACA 65-100.*

5. Conclusion

5.1 The transonic flow

The computed mesh *Fig. 5* was refined after adaptations in the area of the shock wave and along a part of the upper profile of the compressor blade cascade from the shock wave to almost the trailing edge in *Figs. 6, 7*. A flow field could be explored by contours of the Mach number in *Fig. 4*. Flowing accelerate from the inflow to the shock wave. The supersonic flow is found in front of and around the shock wave. Subsonic flow is found behind the shock wave towards outflow where the flowing is slowdown. Between the supersonic and the subsonic flow, so behind the shock wave towards the trailing edge, is found the transonic flow. The flow field matches with the character of the compressor blade cascade.

Figs. 8, 9 illustrate clearly that between vectors heading against each other is one vector heading up. Turning of vectors against each other is characteristic for a separation. The adaptation over boundary was performed to know if the separation was happened. The separation of velocity vectors behind the shock wave hadn't happened *Fig.10*. So velocity vectors are leaving the flowed profile on the trailing edge.

Figs. 11, 12 show that the density ρ = 1.27 [kg.m^{-3}] and the pressure p = 111000 [Pa] are reaching maximum values at the leading edge. The Mach number *Fig. 4* reached the maximum value M = 1.47 [-] in the area of the shock wave. By the comparison of values of the Mach number, from the computation (*3*) on the outflow M = 0.574 [-] with the output value M = 0.59 [-] from the graphics output in *Fig. 4*, can be said that the performed computation by the program *ANSYS Fluent v12* is correct.

5.2 The transition model

The most unsteady behavior for the laminar flow *Fig. 13* can be seen from the RMS velocity magnitude which shows the largest deviation of a steady flow. The blue area is approaching to the steady state and the red area is approaching to the unsteady state. The point on the upper profile between that states can be important for a next review with another factors and for an investigation of the separation despite on the fact that the separation doesn't depend on the steady state.

Unsteady behaviors of the static pressure of the laminar flow *Fig. 14* have the lowest maximum value from the transition model. The maximum value of the transition model has the standard model of turbulence p = 4550 [Pa] what could means that this model is not accurate compare to the advance model which has almost the same value as the laminar flow.
From the *Figs. 23, 24* are seen values of the Wall Yplus which don't go over the value 45. It's commonly known that values for the turbulent flow the Wall Yplus should be under 60. The law of the wall says that in some definite point of a turbulent flow is the average velocity adequate to the logarithm of the distance from that point to the wall (y+). The wall coordinate Yplus is the distance to the nearest wall multiplied by friction velocity at the nearest wall and overall divided by kinematic viscosity.
The unsteady behaviors of velocity magnitude of the laminar flow *Fig. 17* show a vortex street behind the trailing edge and a possible separation of the boundary layer. The *Fig. 18* shows vectors of velocity which show the backward flow without the stagnation flow. The boundary layer is separated from the profile and after is attached to the profile. In this area is found the separation bubble. Also in the boundary layer in front of the separation bubble the flow is turned back. The reattachment of the boundary layer is also shown on the *Fig. 21* by the wall shear stress. Since the boundary layer is attached after separation so the separation bubble is denoted as the closed separation bubble. The separation can be determined also by the wall shear stress *Figs. 21, 22*. When the behaviors touch the zero value of the wall shear stress the flow is separated and is leaving the profile if the flow hadn't been attached again.
For the laminar flow it has seems that the flow was separated and attached to the boundary layer at least two times on the upper profile and is leaving the profile on the trailing edge. The turbulent flow wasn't separated or reattached and is leaving the profile on the trailing edge.
The transition from the laminar flow to the turbulent flow on the advance turbulent model is seen on *Figs. 25, 26*. The transition, e.g., of the upper profile in the position nearby x = 0.05 [m] could be also found and determined by a slight vibration at the same position of the wall shear stress characteristics on the *Fig. 26.*
The laminar flow has an unsteady structure with the closed separation bubble, which will maybe have an effect on the transition. The turbulent flow of the standard model has fine steady structure and the separation hadn't happened. The turbulent flow of the advance model showed that on a collocation of the intermittency was the transition evoked by instability in the boundary layer. The transition is denoted as the bypass transition. The base conception was confirmed so the boundary layers of the turbulent flow are less sensitive to a separation.

Nomenclature

a	Sound velocity	[m.s^{-1}]
c	Body velocity	[m.s^{-1}]
E	Total energy	[J]
$\vec{F}$	Force vector	[N]
$\vec{g}$	Gravitational acceleration	[m.s^{-2}]
h_j	Enthalpy of species j	[J.kg^{-1}]
$\vec{J}_j$	Diffusion flux vector of species j	[kg.m^{-2}.s^{-1}]
k_{eef}	Effective conductivity	[W.K^{-1}.m^{-1}]
M	Mach number	[-]
p	Static pressure, output pressure	[Pa]
p_0	Input pressure	[Pa]
r	Specific gas constant	[J.kg^{-1}.K^{-1}]
S_h	Source of the heat of chemical reaction and any other	[kg]

	heat volumetric sources defined by user	
S_m	Source of the mass added to the continuous phase from the dispersed second phase (e.g., due to vaporization of liquid droplets) and any other user-defined sources	[kg]
T	Temperature, output temperature	[K]
T_0	Input temperature	[K]
t	Time	[s]
$\vec{v}$	Overall velocity vector	[m.s^{-1}]
κ	Adiabatic ratio	[-]
ρ	Density	[kg.m^{-3}]
$\bar{\bar{\tau}}$	Stress tensor	[Pa]
$\bar{\bar{\tau}}_{eef}$	Effective tensor	[Pa]

Shortcuts

ANSYS Fluent	Program for general purpose of *CFD* code based on the finite volume method on collocated grid
AP	Analysis / Direct Problem
Aspect ratio	Factor evaluating elongation of cells
CFD	Computational Fluid Dynamics
Density based	The *ANSYS Fluent* mode for compressible flow
DP	Design / Inverse Problem
Equisize skew	Factor evaluating skewness of cells
Gambit	Pre-processor of the program *ANSYS Fluent* using for creating geometry and generating grid
NACA	National Advisory Committee for Aeronautics
NACA Airfoils	Airfoil shapes for aircraft wings developed by *NACA*
NACA Cowling	Types of aerodynamics fairing use to streamline of radial engines for airplanes developed by *NACA*
NACA Duct	Low-drag intake design mostly for automotive industry developed by *NACA*
NASA	National Aeronautics and Space Administration
PIV	Particle Image Velocimetry
Pressure based	The *ANSYS Fluent* mode for incompressible flow
RNG k-ε model	Mathematic method to inference model of turbulence, e.g., similar to *k* - *ε* re-normalization group of Navier-Stokes equations
Size change	Factor evaluating size change of neighboring cells
Skewness	Factor evaluating skewness of cells
SST transition model	Shear stress transport model provides generally the most accurate calculation of turbulence model
TGrid	Generator for creating unstructured mesh from defined surface mesh

References

[1] AS CR: Documentation of the compressor blade cascade NACA 65-100, Institute of Thermomechanics of the ASCR, v.v.i., 2008

[2] ANSYS, Inc.: ANSYS FLUENT 12 - Documentation, 2008

[3] Citavý J., Nožička J.: Lopatkové mříže; Vydavatelství ČVUT, Praha, 2003

[4] Nožička J.: Mechanika tekutin, Nakladatelství ČVUT, Praha, 2006

[5] NASA: NASA History Division, <http://www.history.nasa.gov/naca>, 2009